

# JOURNAL OF NEW TECHNOLOGIES IN ENVIRONMENTAL SCIENCE

No. 3    Vol. 6    ISSN 2544-7017    www.jntes.tu.kielce.pl    Kielce University of Technology

## CONTENTS

Vyacheslav KREMNOV, George BELYAEV, Konstantin ZHUKOV, Natalya KORBUT, Leonid SHPILBERG, Valentina STETSUK, Andriy TIMOSHCHENKO <b>FIRE SAFE STORAGE AND PRELIMINARY DEHYDRATION OF WOOD WASTE WITH DIAMETER &lt;30 MM FROM FINAL FELLING AND FOREST CARE FELLING, AS A SEMI-FINISHED PRODUCT FOR THE PRODUCTION OF SOLID FUEL</b> .....	85
Volodimir DEMCHENKO, Alina KONYK <b>MOBILE THERMAL ENERGY STORAGE (M-TES)</b> .....	91
Borys BASOK, Oleksandr NEDBAILO, Ihor BOZHKO, Volodymyr MARTENIUK <b>ANALYSIS OF THERMOTECHNICAL PARAMETERS OF AIR-WATER HEAT PUMP AS A PART OF THE RADIATOR SYSTEM OF HEAT SUPPLY OF THE ADMINISTRATIVE BUILDING</b> .....	97
Andrii CHEILYTKO <b>INFLUENCE OF STRUCTURAL CHARACTERISTICS OF POROUS MATERIALS ON THE COEFFICIENT OF THERMAL CONDUCTIVITY</b> .....	104

**Editor-in-Chief:**

prof. Lidia DĄBEK – Faculty of Environmental, Geomatic and Energy Engineering,  
Kielce University of Technology (Poland)

**Associate Editors:**

prof. Anatoliy PAVLENKO – Faculty of Environmental, Geomatic and Energy Engineering,  
Kielce University of Technology (Poland)

**Board:**

prof. Anatoliy PAVLENKO – Kielce University of Technology (Poland)

prof. Lidia DĄBEK – Kielce University of Technology (Poland)

prof. Hanna KOSHLAK – Kielce University of Technology (Poland)

**International Advisory Board:**

prof. Boris BASOK, academician of the NAS of Ukraine – Institute of Engineering Thermophysics National  
Academy of Sciences of Ukraine

prof. Mark BOMBERG – McMaster University (Canada)

prof. Jan BUJNAK – University of Žilina (Slovakia)

prof. Valeriy DESHKO – National Technical University of Ukraine “Igor Sikorsky Kyiv Polytechnic Institute” (Ukraine)

prof. Ejub DZAFEROVIC – International University of Sarajevo (Bosnia-Herzegovina)

prof. Andrej KAPJOR – University of Žilina (Slovakia)

prof. Engvall KLAS – KTH (Sweden)

prof. Vladymir KUTOVOY – Harbin Institute of Technology (China)

prof. Ladislav LAZIĆ – University of Zagreb (Croatia)

prof. Zhang LEI – Faculty of Thermal Engineering, CUPB University of Oil and Gas (China)

prof. Milan MALCHO – University of Žilina (Slovakia)

prof. Violeta MOTUZIENĖ – Vilnius Gediminas Technical University (Lithuania)

prof. Łukasz ORMAN – Kielce University of Technology (Poland)

prof. Jerzy Z. PIOTROWSKI – Kielce University of Technology (Poland)

prof. Miroslav RIMÁR – Technical University of Košice with a seat in Prešov (Slovakia)

prof. Ibragimow SERDAR – International University of Oil and Gas (Turkmenistan)

[www.jntes.tu.kielce.pl](http://www.jntes.tu.kielce.pl)

[jntes@tu.kielce.pl](mailto:jntes@tu.kielce.pl)

The quarterly printed issues of Journal of New Technologies in Environmental Science are their original versions.  
The Journal published by the Kielce University of Technology.

ISSN 2544-7017

Doi: 10.53412

© Copyright by Wydawnictwo Politechniki Świętokrzyskiej, 2022



Vyacheslav KREMNOV, George BELYAEV  
Konstantin ZHUKOV, Natalya KORBUT  
Leonid SHPILBERG, Valentina STETSUK  
Andriy TIMOSHCHENKO

*Institute of Engineering Thermophysics of NAS Ukraine  
2a Marii Kapnist Str., Kyiv, 03057, Ukraine*

Corresponding author: kremnev@ukr.net

Doi: 10.53412/jntes-2022-3-1

## FIRE SAFE STORAGE AND PRELIMINARY DEHYDRATION OF WOOD WASTE WITH DIAMETER <30 MM FROM FINAL FELLING AND FOREST CARE FELLING, AS A SEMI-FINISHED PRODUCT FOR THE PRODUCTION OF SOLID FUEL

**Abstract:** *The purpose of the work was to obtain fairly reliable initial data regarding the organization of fire-safe long-term storage of wet wood waste of a small diameter in the open air by various alternative methods. The subject of research was freshly felled hardwood with leaves in the form of a mixture of the following botanical composition: poplar, maple, cherry, mulberry. The average moisture content of freshly cut wood is 50%, i.e. 1 kg of moisture per 1 kg of completely dry wood. The three most common ways of storing of wet wood waste with diameter  $\leq 30$  mm were researched. In its natural form – in a pile and a fragment of a stack, and in its chopped form – in the form of wet "green" chips. During the storage period, the moisture content decreased on average: in the pile ~ by 5 times; in the stack fragment – 4.3 times; in a fragment of a stack of the "green" wood chips of trapezoidal section ~2.5 times [1, 2].*

**Keywords:** *storage, wood waste from felling, wet "green" wood chips, preliminary dehydration, semi-finished fuel.*

### Introduction

Involvement in the fuel use of waste from felling for forest care and main use requires the organization of safe storage of large volumes of wet wood resources. The category of waste, in accordance with the regulatory documentation of Ukraine, includes tops of trunks and branches with a trunk diameter of <30 mm. According to the rules, these resources are subject to destruction by burning with using of liquid fuel in specially designated places. For fire safety reasons, this is done in the fall. In addition to the destruction of such waste by burning, it is allowed to grind it into wood chips and scatter it between trees for natural, gradual degradation. This method of destruction is considered undesirable due to wood chips disrupting natural biological processes in the forest floor, which plays an important role in the forest biocenosis. Currently, there is no established system of cooperation and coordination between forestry and energy in Ukraine. In our opinion, such a system is very necessary and must necessarily have a synergistic, mutually beneficial character – that is, promote the development of both forestry and energy. Wood fuel fully meets modern environmental requirements, is a promising renewable resource, but requires large volumes of raw material storage. For example, compared to coal, taking into account the difference in calorific value, bulk mass and humidity, the volume of wood in warehouse cubic meter exceeds the volume of coal by approximately 20 times, assuming the same thermal energy potential.

At the Institute of Engineering Thermophysics, within the framework of the topic "Research of heat and mass transfer processes and the development of new energy-efficient methods and technological equipment for the production of biofuel from forestry waste", the harvesting of small-diameter wood together with green leaves was carried out, as well as the storage of this wood for 16 months.

So, the storage of small-diameter wood in the three most common ways was researched, namely: in its natural form – in a pile and a fragment of a stack, and also after chopping wood – in the form of wet "green" chips (Fig. 1). The first and second methods are considered safe in terms of self-ignition, so the main task of researching these methods was the effect of long-term storage on the moisture content of wood. The third method – in the form of wet wood chips is considered dangerous in terms of self-ignition, and this especially applies to "green" chips obtained by the method of chopping wood together with leaves.

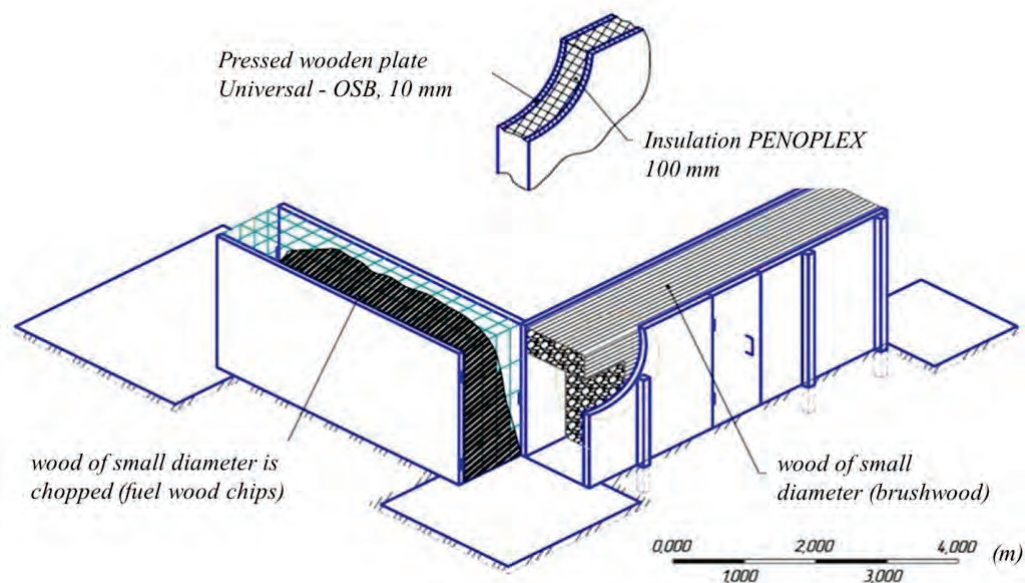


**FIGURE 1.** Structural scheme of the building for experimental research long-term storage and preliminary drying wood

### **Characteristics of alternative methods of outdoor storage for 16 months**

1. In a separate pile, in the form of whole trees with leaves: width – 1.7 m; length – 3.4 m; height – 1.5 m; bulk volume  $\sim 9 \text{ m}^3$ .
2. In a fragment of an industrial stack: width – 5 m; height – 2 m; length – 1 m (in practice, the length is not limited, has no technological significance and is determined for organizational reasons, taking into account the size and shape of the storage area); bulk volume  $\sim 10 \text{ m}^3$ .
3. A fragment of the stack of crushed wood together with "green" leaves (of the "green" chips). Stack dimensions: height – 2 m; width: at the mark "0" – 5 m, at the mark "2" – 3 m; length – 1 m; bulk volume  $\sim 5.5 \text{ m}^3$ .

The conception (idea) of the research was based on the following:

- Pile storage was organized on a 1:1 scale and is a full-scale experimental and industrial test.
- Storage of freshly cut "green" wood in a stack is organized in the form of a 1 m long fragment with a cross-section on a scale of 1:1, which had the shape of a rectangle, 5 m wide and 2 m high. The fragment of the stack was formed between two parallel heat-insulated flat fences.
- The research of wet "green" chips was aimed, first of all, at determining the technical conditions that prevent spontaneous combustion, which has repeatedly occurred in practice and was confirmed by researchers from different countries.

When choosing the shape and cross-sectional dimensions of the stack for storing wood chips, we took the following into account:

- Self-ignition requires a temperature level that cannot be achieved only through purely biochemical processes. Reaching the temperature necessary for self-ignition indicates the participation of exothermic chemical reactions (probably hydrocarbon oxidation reactions in the presence of flammable gases).
- Flammable gases can be formed during the activity of facultative microflora, which operates at an oxygen concentration insufficient for aerobic microflora, which produces only non-flammable gases – water vapor and carbon dioxide.

The above considerations indicate a huge unevenness of conditions in the massif of "green" wet cod. Similar problems associated with insufficient aeration occur during composting of biomass – its biological conversion by fermentation under the influence of aerobic microflora. In field composting technology, this problem is solved by mixing and aerating biomass with specialized mechanisms. Therefore, we decided to organize the storage of wet "green" wood chips in a fragment of an elongated stack with cross-sectional dimensions that would allow, if necessary, processing of the stack with commercially available mixer-aerators.

A 1 m long stack fragment was arranged between two parallel heat-insulated flat fence walls with a cross-section in the form of a trapezoid. Section dimensions: height – 2 m; width: at the "0m" mark – 5 m, at the "2m" mark – 3 m; length – 1 m.

During the entire period of storage, the temperature was measured at different points of the internal volume of the wood using a specially designed probe (Fig. 2).

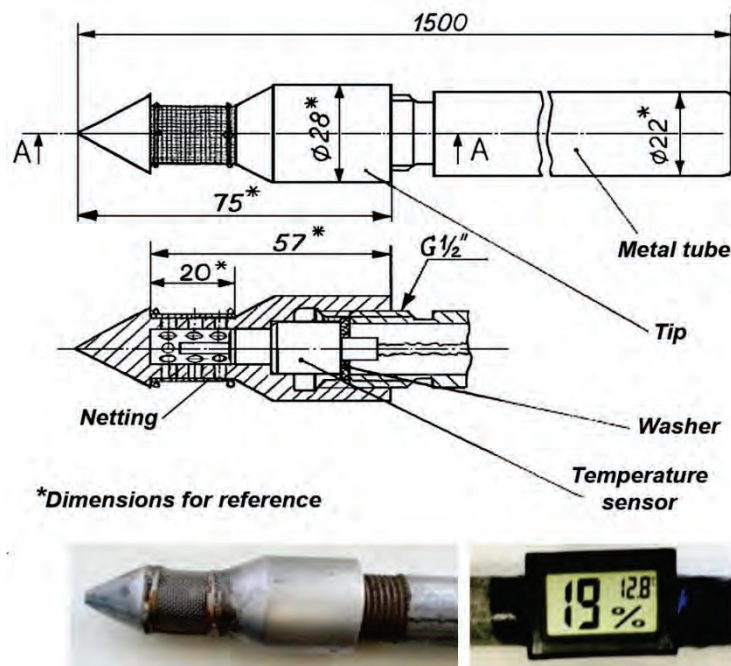


FIGURE 2. Immersion temperature measuring device – "probe" 1500 mm long

The probe provides measurement of the air temperature in the location area of the mechanically protected sensor. Air is a continuous gaseous phase in the inner volume of a two-phase material. The solid phase of the material is represented: in the pile and stack by whole brushwood with leaves, and in the chip stack by polydisperse fragments of wood (chips) and leaves.

It was established that the temperature in the massif of the heap was almost no different from the ambient temperature; in the stack fragment it reached 40°C; the maximum temperature in the chips massif reached 62°C, after which it gradually decreased to the ambient temperature over the course of 2 months.



During the storage period of the raw material, its moisture content decreased on average:

- In a pile ~5 times (from 1 kg of moisture per 1 kg of completely dry wood to 0.2 kg of moisture per 1 kg of completely dry wood) (Figs. 3, 4).



**FIGURE 3.** Storage in a separate pile

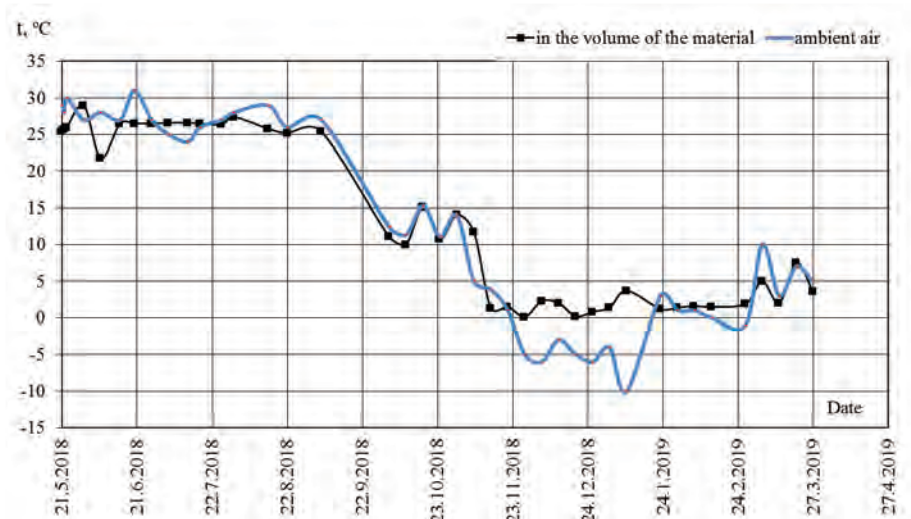


**FIGURE 4.** Temperature in the material pile and the environment

- In a stack fragment – 4.3 times (from 1 kg of moisture per 1 kg of completely dry wood to 0.23 kg of moisture per 1 kg of completely dry wood) (Figs. 5, 6).



**FIGURE 5.** Experimental fragment of the stack

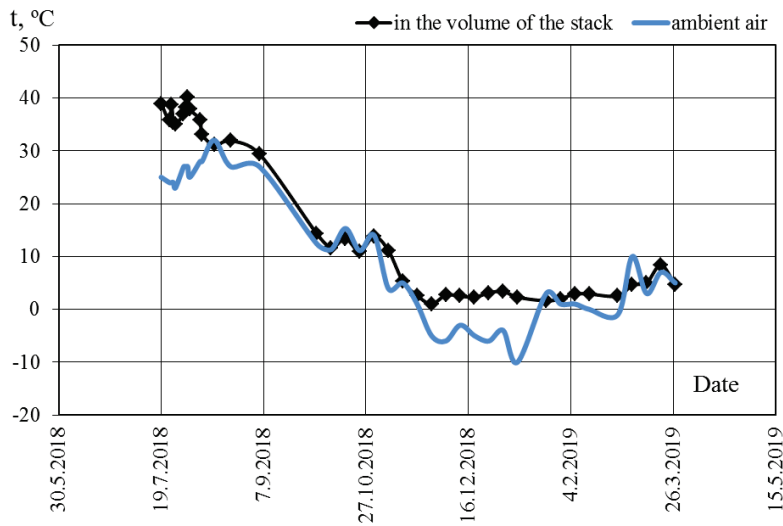


FIGURE 6. Temperature in the volume of the stack fragment and the environment

- In a fragment of a stack of "green" wood chips ~2.5 times (from 1 kg of moisture per 1 kg of completely dry wood to 0.4 kg of moisture per 1 kg of completely dry wood) (Figs. 7, 8).



FIGURE 7. Fragment of a stack of "green" wood chips

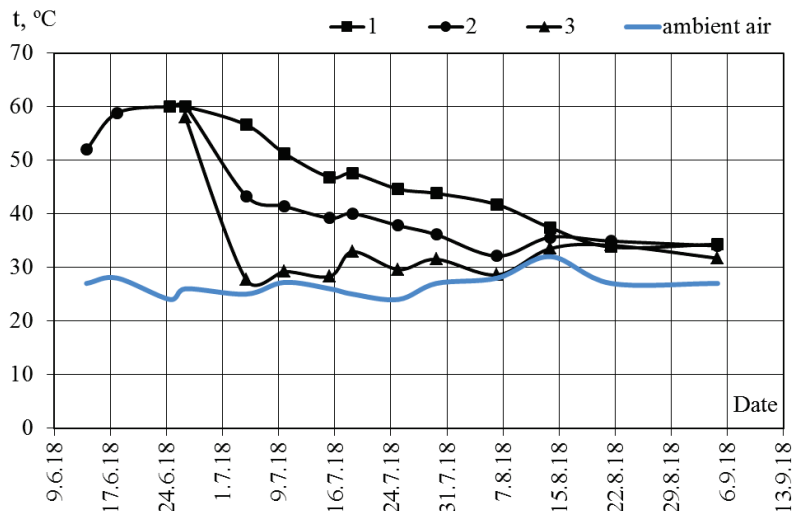


FIGURE 8. Temperature in the environment and in the volume of the wood chips (points 1, 2, 3)

## Discussion

In our opinion, some advantage in the dewatering of whole wet wood waste  $\leq 30$  mm in diameter when stored in a pile, compared to stored in a stack, is explained by the following factors:

- a larger specific external surface in relation to the environment;
- better air exchange conditions.

When storing whole wet wood waste with a diameter  $\leq 30$  mm in a pile, the effect of biological conversion is not noticeable, as evidenced by the practical temperature equilibrium with the environment.

When storing whole wet wood waste with a diameter of  $\leq 30$  mm in a stack, there is some influence on the dehydration of the biological conversion process, which is evidenced by reaching a temperature of  $40^{\circ}\text{C}$ .

The study of long-term storage of "green" wood chips proves that a very active process of biological conversion takes place in its volume. This is evidenced by reaching a temperature of  $62^{\circ}\text{C}$ . Such an increase in temperature is characteristic of the so-called succession process. With it, there is a gradual change in microflora generations (cryophilic generation –  $10\text{-}20^{\circ}\text{C}$ , mesophilic –  $20\text{-}40^{\circ}\text{C}$ , thermophilic –  $40\text{-}65^{\circ}\text{C}$ ).

Such a scheme of gradual change of generations of microflora is characteristic of composting (solid-state microbial fermentation). At each stage, the next generation of microflora utilizes the previous microflora as an edible medium. Reaching a temperature  $\geq 60^{\circ}\text{C}$  practically stops the processes of biological conversion.

## Conclusions

1. All researched storage methods are safe with respect to spontaneous combustion.
2. Long-term storage ( $\geq 16$  months) provides significant dehydration; when stored whole wet wood waste with a diameter of  $\leq 30$  mm in a pile and stack, it is practically provide that the air-dry state is reached, and the fuel semi-finished product does not require further dehydration. Storage in the form of fuel chips requires further drying of the semi-finished product.
3. Dehydration during storage in the form of wet "green" wood chips is ensured mainly due to the process of biological conversion of shredded leaves and small wood particles. We formulated and received a patent for a useful model for stacking wet wood chips in elongated stacks of a defined cross-section, which is sufficient for fire-safe storage and significant preliminary drying without stirring [3]. In addition, acceleration (if necessary) of conversion and drying by mixing and aeration was proposed.

## References

- [1] Kremnev V., Lyashenko A., Korbut N., Shelimanova E., 2019, *Development of a method of fire-safe long-term storage and partial dehydration of wood chips*. Enerhetyka i avtomatyka, 6, pp. 202-213. <http://dx.doi.org/10.31548/energiya2019.06.202> (Ukr).
- [2] Kremnev V., Timoshchenko A., Korbut N., Shelimanova E., 2019, *Organized long-term storage and pre-driving of nonliquid wood (twigs and shrub) in open air under the influence of natural factors*. Enerhetyka i avtomatyka, 6, pp. 111-121. <http://dx.doi.org/10.31548/energiya2019.06.111> (Ukr).
- [3] Kremnev V., Timoshchenko A., Shpilberg L., Zhukov K., Korbut N., 2020, *A method of long-term storage of wet fuel wood chips made of thin gauge wood. Patent of Ukraine for useful model*. F26B 9/00 C10L 5/00 C10L 5/40. №142712, declared 11.12.2019; published 25.06.2020, № 12. (Ukr).



Volodimir DEMCHENKO

Alina KONYK

Institute of Engineering Thermophysics of the NAS of Ukraine

Corresponding author: Alina\_tds@ukr.net

Doi: 10.53412/jntes-2022-3-2

## MOBILE THERMAL ENERGY STORAGE (M-TES)

**Abstract:** *The main world trends aimed at creating new energy systems, highly efficient and, at the same time, with a careful attitude to the surrounding environment, intensified the creation and protection of energy storage systems. One of the areas that is actively developing is mobile heat accumulators that work on this technology of latent heat storage.*

*The article presents a new design of a mobile heat accumulator with a short-term heat storage period. A combination of several types of coolants is used as an accumulation system. The technical and technological characteristics of M-TES-0.5 MW are given. The most promising mobile thermal energy storage devices, which implement a similar principle of thermal energy conservation and have a positive experience of use, were noted.*

**Keywords:** *thermal energy storage, mobile thermal energy storage, phase change material.*

### Introduction

In countries with developed economy, there is a transition to smart energy consumption that is accompanied by the development of technologies with a careful attitude to natural resources and the surrounding environment. Energy-efficient technologies are being used, new equipment, automation and measuring equipment are being created. They reduce the cost of electrical and thermal energy. The main changes concern (Wirtza et al., 2020; Thermal networks, 2008; Union European. EU Energy in figures: Statistical pocketbook, 2020; Lunda et al., 2017; Lunda et al., 2014) with:

- lowering the heat carrier temperature;
- reduction of heat losses at each stage of heat supply;
- attraction of new non-traditional energy sources;
- creation of decentralized heat supply.

One of the technological solutions used in almost each of these issues is the conservation and accumulation of heat. Nowadays heat storage technologies, special equipment and materials are actively developing (Zayeda et al., 2020; Levenberg et al., 1991; Demchenko et al., 2020). The paper is devoted to the development of mobile heat accumulators operating based on latent heat technology (Guo et al., 2014; Du et al., 2020).

Within the framework of the state order in the Institute of Engineering Thermophysics of National Academy of Sciences of Ukraine design documentation for Mobile Thermal Energy Storage (hereinafter M-TES) for transporting heat from various energy sources has been developed. As a result of the work carried out, M-TES with a heat output of 0.5 MW was manufactured and tested.

The design of the M-TES has several of original and at the same time universal solutions presented as objects of patents for inventions:

- design of the battery tank (patent application a2019 11450, patent No. 126579 dated 02.11.2022);
- the composition of the heat storage material used in the storage tank to increase the storage effect (patent application a2021 07588);
- design of the M-TES system as a whole (patent application a2021 01559).

The main purpose of using M-TES is to ensure the collection and primary processing of initial information; create a unified reporting system on performance indicators; improve the quality (completeness, accuracy, reliability, timeliness, consistency) of information; reduce the processing time of information thermal processes, the safety of information and fire safety.

### **Purpose and objectives of the work**

The purpose of this work is to present a new design and review the design features of mobile thermal energy storage that work on the technology of hidden heat storage.

In accordance with the set goal, the following tasks are formulated:

- presentation of a new design of M-TES with a short-term accumulation cycle;
- consider the existing designs of M-TES and determine promising directions for the development of this industry.

### **Mobile thermal energy storage**

The mobile thermal energy storage is a reliable universal design housed in a standard 20-foot Dry Cube "20DC" container. The container structure is equipped with roller shutters made of AG77 profile, namely, a system for closing technological openings. To insulate the containers in the container, liquid ceramic latex thermal insulation is used.

The container is divided by a partition into two parts an accumulation zone and an individual heating point (IHP).

The accumulation zone consists of 8 heat accumulators (hereinafter referred to as the HA) installed in containers in 2 rows. In the first row 4 heat accumulators are connected in series with each other, in the second row 4 heat accumulators are connected in parallel (Fig. 1). Each HA is equipped with temperature and pressure sensors. Charging and discharging of HA is carried out with the help of IHP.

The operation of the IHP is carried out through the entrance gate of the container. The ITP is not supposed to have a permanent stay of personnel. For remote monitoring and control the MTE-S is equipped with a PRO-X multifunctional GSM controller (OKOTM, Ukraine), which is usually used for remote monitoring and management at stationary objects simultaneously performing a number of functions.

To ensure adequate operation of the equipment, the M-TES is equipped with a modern automatic control system. The purpose of the automation system is to provide control of the heat supply process with the help of M-TES, access to information about its verification. Therefore, the system must be able to perform the following tasks:

- simplification of data entry;
- providing a secure authentication protocol for logging into the system;
- prevention of user errors when entering data;
- ensuring secure storage of entered data;
- providing open online access and search tools for open data located in the public module and the possibility of downloading them;
- creating an open API for developers to provide secure access to open data and download it in different formats.

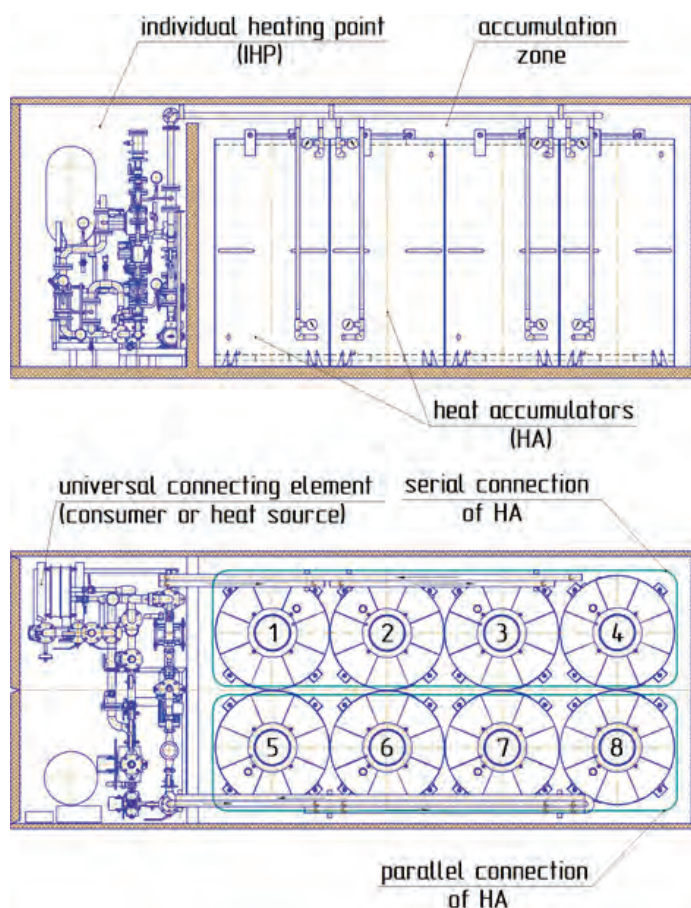


**FIGURE 1.** Mobile thermal energy storage M-TES-0.5 MW

To ensure the operation of M-TES the following are automated:

- temperature regulation of supply and return pipelines from the consumer and the storage module;
- management of M-TES charging and discharging processes;
- registration of unauthorized access and fire safety of M-TES;
- the geographical location of M-TES.

### Technical characteristics of M-TES-0.5 MW

When creating M-TES-0.5 MW, a set of working design documentation was developed. Namely, there are Terms of Reference, Passport, Specifications, a set of working and design documentation. The main technical parameters of these documents are presented in Table 1.

**TABLE 1.** Technical characteristics of M-TES-0.5 MW

Parameter, unit of measurement	Value
Mode of operation of M-TES	cyclic
Thermal capacity of M-TES, MW, no more than	0.5
Pressure in tanks and pipelines of the accumulated compartment, MPa, no more than	0.07
Productivity of the heat carrier of the heating/cooling circuit, m <sup>3</sup> /h, up to	2.5
Electric power installed, kW, no more than	8.2

table 1 continued

Parameter, unit of measurement	Value
The temperature of the heat carrier in the heat accumulator circuit when: – charging, °C – discharging, °C	90 50
The temperature of the direct heat carrier during M-TES charging, °C The temperature of the return heat carrier during M-TES charging, °C	110 60
The temperature of the direct heat carrier during M-TES discharging, °C The temperature of the return heat carrier during M-TES discharging, °C	50 30
The volume of the heat carrier in the heat accumulator, m <sup>3</sup> , up to	1.5
The volume of the heat carrier in M-TES as a whole, m <sup>3</sup> , up to	12
Overall dimensions of M-TES, no more than – length, mm – width, mm – height, mm	6300 3000 3000
Air temperature in the environment during operation, °C	-10.....-15

The operation mode of M-TES can be intermittent, periodic or cyclical depending on the type of heat source, consumer conditions and the distance between them.

### Overview of implemented projects based on mobile energy transportation

In the last 20 years, up to 100 projects using M-TES have been implemented in Europe, the USA, China and Japan. Let's consider the main aspects of some of them – Table 2.

TABLE 2. Global experience of creating M-TES







Heat productivity	PCM	Heat source	Consumer	Transportation distance	Developer	Construction of M-TES
200 kW/h	Acetate trihydrate	Any one with a temperature up to 115°C	–	–	Institute Fraunhofer UMSICHT	
2.3 MW/h	Zeolite (14 tons)	Steam from the incineration plant	To charge the storage of hot air 130°C and the drying process	7	Research center ZAE Bayern	
4 MW-h	Barium hydroxide (25 m <sup>3</sup> , LSG Sky Chefs)	Used warm from a power plant)	Kitchen power plant	–	LSG Sky Chefs, Cologne	



table 2 continued

Heat productivity	PCM	Heat source	Consumer	Transportation distance	Developer	Construction of M-TES
-	-	Spent steam of the SANYO electronics factory	Pre-heating of the boiler reverse water	20	Osaka, Japan	
-	-	Heat collected from counters in Kiyose	City gymnasium	2.5		
-	-	Disposal of exhaust gases from the annealing furnace of the steel plant in Osaka	Public bath	3		
6.5 GJ	HECM-WD03 with the addition of rare earth elements	Waste heat of the steel plant in Dalyana	Neighboring hotels	-	Zhongyineng (Beijing) Technology Co, China	
-	-	Used steam of the power plant	Heating a neighboring school	-	Qingdao Aohuan New Energy Group Co., Ltd., China	

First, heat transportation by road transport is economically feasible only if 3 factors are met:

- a small distance from the heat source to the consumer, usually within 50 km;
- availability of an available source of energy, for example, waste heat of enterprises, etc.;
- the temperature of the heat carrier is high enough to ensure the temperature range of M-TES operation.

Secondly, the determining limiting factor for the application of M-TES is the existing legal framework that regulates the safety of transportation and the economic basis for payment settlements.

## Conclusions

As a result of the conducted research and experimental work, the following results were obtained:

1. A universal design of M-TES-0.5 MW has been developed, in comparison with existing M-TES, which has a number of original technical solutions aimed at obtaining the maximum possible coefficient of heat storage.
2. In the design of M-TES to increase heat transfer, the complex use of heat carriers – PCM, a water-based material with water-soluble polymers.
3. The optimal composition of a mixture of high-molecular solid saturated hydrocarbons and water-soluble polymers for intensifying the heat accumulation process was selected and laboratory researched, which made it possible to increase the specific heat capacity of TAM by 30% and expand the range of its use from -10°C to +120°C.
4. Approbation and field tests of the M-TES prototype with a thermal capacity of 0.5 MW proved that their implementation can fundamentally change the heat supply paradigm and in a short time introduce a 4th generation centralized heat supply system in Ukraine.

## References

- Wirtza M., Kivilipa L., Remmena P., Mullera D., 2020, *5th Generation District Heat-ing: A novel design approach based on mathematical optimization*, Applied Energy, 260. DOI: <https://doi.org/10.1016/j.apenergy.2019.114158>.
- Thermal networks (2008), DBN B.2.5-39: 2008, Valid from 2009-01-07 [Heating networks, DBN B.2.5-39: 2008, in force since 2009-01-07].
- Union European. EU Energy in figures: Statistical pocketbook 2020. 2020. URL, <https://op.europa.eu/s/oIDP>. DOI:10.2833/75283.
- Lunda H., Østergaard P.A., Connolly D., Mathiesen B.V., 2017, *Smart energy and smart energy systems*, Review. Energy, 137. 556-565 DOI: <https://doi.org/10.1016/j.energy.2017.05.123>.
- Lund H., Werner S., Wiltshire R., Svendsen S., Thorsen J.E., Hvelplund F., et al., 2014, *4th Generation District Heating (4GDH): integrating smart thermal grids into fu-ture sustainable energy systems*. Energy, 68. 1-11. DOI: <https://doi.org/10.1016/j.energy.2014.02.089>.
- Zayeda M.E., Zhaoa J., Lia W., Elsheikhc A.H, Elbannab A.M., Jinga L., Geweda A.E., 2020, *Recent progress in phase change materials storage containers: Geometries, design considerations and heat transfer improvement methods*. Energy Storage, 30. DOI: <https://doi.org/10.1016/j.est.2020.101341>.
- Levenberg V.D., Tkach M.R., Holström V.A., 1991, *Heat accumulation*. Technique, p. 111.
- Demchenko V., Konyk A., 2020, The main aspects of the processes of heat-akumulation Scientific Works, 84(1), 48-53. [Demchenko V.G., Konyk A.V., Main aspects of heat-acumulation processes, Odessa National University of Food Technologies, Collection "Scientific Proceedings", 2020. Issue 1, Vol. 84, pp. 48-53. DOI: <https://doi.org/10.15673/swonaft.v84i1.1868>.
- Guo S., Li H., et. al., 2014, *Experimental study on the direct/indirect contact energy storage container in mobilized thermal energy system (M-TES)*. Applied Energy, 119, pp. 181-189. DOI: <https://doi.org/10.1016/j.apenergy.2020.116277>.
- Du K., Eames P., Kaiser J., Calautit S., Wu Y., 2020, *A state-of-the-art review of the application of Phase Change Materials (PCM) in Mobilized-Thermal Energy Storage (M-TES) for recovering lowtemperature Industrial Waste Heat (IWH)*. Renewable Energy. DOI: <https://doi.org/10.1016/j.renene.2020.12.057>.

Borys BASOK<sup>1</sup>, Oleksandr NEDBAILO<sup>1</sup>

Ihor BOZHKO<sup>1</sup>, Volodymyr MARTENIUK<sup>2</sup>

<sup>1</sup> Institute of Engineering Thermophysics of the National Academy of Sciences of Ukraine  
bldg. 2, Bulakhovskogo str., Kyiv, 03164, Ukraine

<sup>2</sup> National University of Food Technologies, 68, Volodymyrska str., Kyiv, 01601, Ukraine

Corresponding author: nan\_sashulya@ukr.net

Doi: 10.53412/jntes-2022-3-3

## ANALYSIS OF THERMOTECHNICAL PARAMETERS OF AIR-WATER HEAT PUMP AS A PART OF THE RADIATOR SYSTEM OF HEAT SUPPLY OF THE ADMINISTRATIVE BUILDING

**Abstract:** The description of original technical decision of using heat pump for heating part of administrating building is described. The hydraulic connection scheme has been developed and selection of heat devices was made for it. The energy efficiency for using heat pump in heating season is analyzed. Based on the obtained experimental data, the coefficient of performance of the heat pump was calculated for the above mode of operation of the heat supply system. With such indicators, a significant saving of thermal energy is achieved in comparison with the use of a centralized heat supply system.

**Keywords:** heat pump, heat supply, coefficient of performance (COP)

### Introduction

According to statistics, people spends up to 90% of the total time in buildings, the climatization of which is comparable to the largest part of the final consumption of all types of energy. In Ukraine, the housing and communal sector uses for more than 40% of this volume, and the efficiency of possible energy-saving measures in this direction, on a national scale, exceeds the possible savings in such technologically energy-intensive industries as metallurgy, chemical industry, etc. [1].

The use of heat pump systems based on renewable energy sources is a real alternative to the use of fossil fuels. More and more attention in the literature has been paid to the issues of efficiency assessment and implementation of heat pump technologies in customer's heat supply systems.

### Literature review

Thus, in [2], the peculiarities of the schematic diagrams of such systems are considered (Fig. 1). The main advantages of using heat pump technologies for heating compared to centralized heat supply are described.

The works [3, 4] describe the concepts and give specific examples of the effectiveness of the use of heat pumps. It is noted that when using heat pump heating systems, the use of energy obtained from fossil carbon fuel is reduced by 2-3 times and the comfortable thermal conditions of a person's stay indoors are significantly improved. Also, at the same time, heat pump systems have less inertia of operation than centralized heat supply systems.

In works [5] it is stated that the higher the coefficient of thermal resistance of enclosing structures, the more profitable the use of heat pump technologies for heating, ventilation and hot water supply of buildings. This is due to the low temperatures of the heat carrier at the output of the heat pump, the transition from radiator heating to water floor heating, as well as the use of accumulator tanks in hot water supply systems.

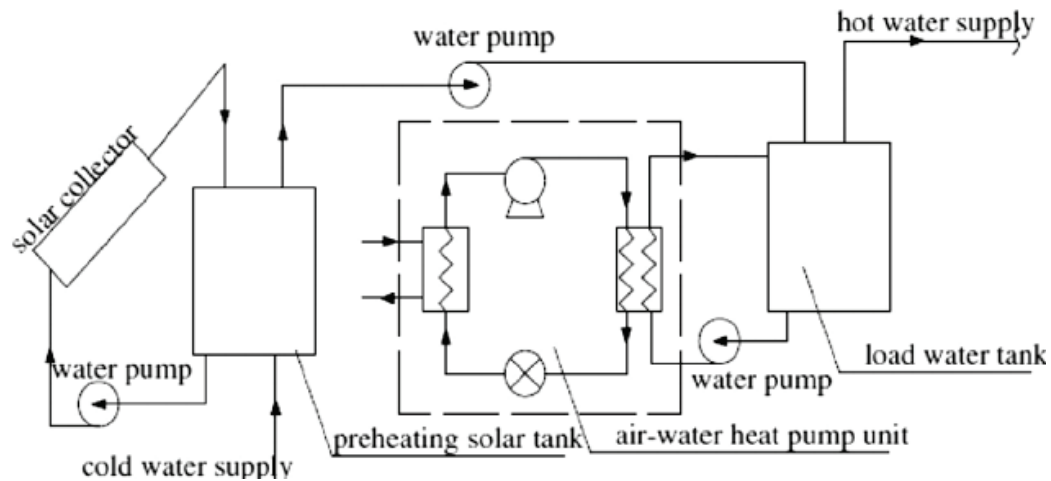


FIGURE 1. Schematic diagram of the combined heat supply system [2]

### Problem formulation

The high energy consumption for the full cycle of building operation in Ukraine is, on average, more than 300 kWh/(m<sup>2</sup>·year) for the heated area, and should be significantly reduced in the future thanks to the widespread implementation of energy-saving measures in the housing and communal economy and increasing energy efficiency of heat supply engineering systems.

### Object, subject, and methods of research

The Institute of Engineering Thermophysics of the National Academy of Sciences of Ukraine has implemented a number of projects aimed on reducing the consumption of thermal energy for the needs of heating of the administrative buildings. Among such projects is the modernization of part of the heating system of building No. 1 of the Institute with the installation of an air-water heat pump [6].

In Figure 2 presents the basic hydraulic scheme of the modernization of the existing centralized heating system of the three-story administrative building of building No. 1 of the Institute using an air-water heat pump. The improvement of the heating system was carried out by integrating the heat pump 7 IVT Optima 1700 (made in Sweden) with an output heat capacity of 16 kW into the existing system of centralized heating of the building [7, 8]. At the same time, the modernized heating system can be operated both from an individual heating station, using heat from the district boiler house, and from a heat pump.

When operating the system according to the first option, in order to avoid contamination of pipelines and heating devices from the heat carrier coming from the heating network, a bubble separator for dirt and gases Spirovent was installed 2.

During the operation of the system from the heat pump, part of the circuit of a typical one-pipe heating system is disconnected from the individual heating station with the help of a shut-off valve. Balancing valves 1 are provided for hydraulic balancing of the circulation along the circuits and prevention of redistribution of the heat carrier in the heating system. Regulation of thermal parameters is carried out according to the temperature of the return water. At the same time, as a result of cutting off part of the heating system, the thermal regime of the building was not disturbed and the maximum effect of energy saving was achieved due to the reduction of the use of heat from the centralized heating network.



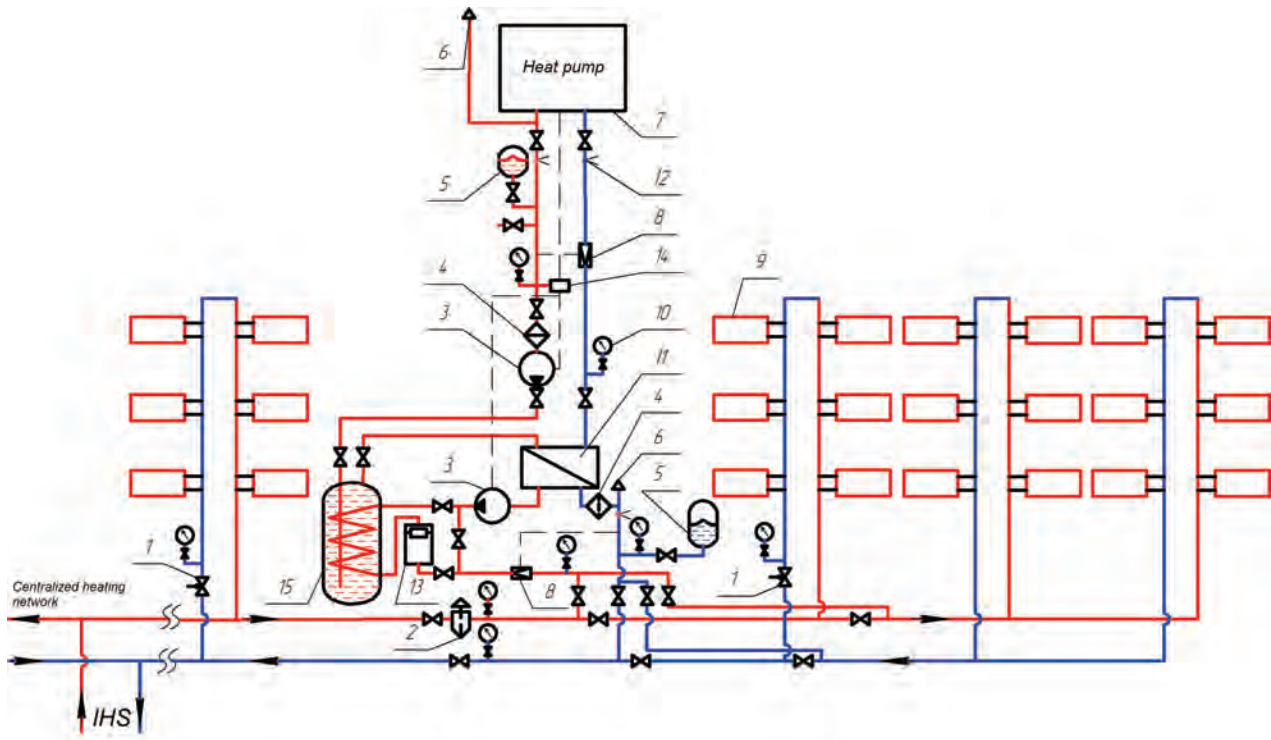


**FIGURE 2.** Schematic diagram of a heating system based on an air-liquid heat pump: 1 – balancing valves; 2 – bubble separator; 3 – circulation pumps; 4 – mesh filters; 5 – membrane expansion tanks; 6 – air vents; 7 – heat pump of the "air-water" type; 8 – heat meters; 9 – radiators of the heating system; 10 – manometer; 11 – plate heat exchanger, 12 – temperature sensor; 13 – electric boiler; 14 – pressure sensor, 15 – accumulator tank; IHS – is an individual heating station

In order to avoid the negative impact of the heat network on the heat pump, hydraulic separation of the heat pump circuit from the heating system circuit through a plate heat exchanger was provided Alfa Laval 10 with the use of an intermediate heat carrier – 20% aqueous solution of ethylene glycol.

At the same time, with the help of the shut-off valves, the fittings of six or four heating circuits (depending on the mode of operation of the heat supply system based on the heat pump) with radiators 9 are disconnected from the centralized heating system.

When filling the circuits and their further operation, air is removed with the help of air vents installed in the highest places of the circuits.

Circulation in both circuits with a given flow rate is provided, respectively, by pumps 3 Wilo-Star-RS 25/6 and Wilo-Top-S 25/10 with heat carrier cleaning by mesh filters 4.

Automatic shutdown of circulation and heat pumps with the help of pressure sensor 14 is provided in case of depressurization of circuits and loss of pressure. To compensate for the volumetric expansion of the heat carrier during its heating, two expansion tanks 5 with a volume of 4 and 50 liters are used, respectively. The volume of the tanks is calculated according to the volume of the heat carrier in the circuit, its coefficient of thermal expansion and the temperature schedule of the heating system. The amount of heat consumed for space heating is measured separately in each of the circuits by heat meters 8 Apator LQM – III – K, which makes it possible to estimate the heat losses in the main pipelines and the efficiency of the heat exchanger. Electric boiler 13 "Eco-Compact" K-6/6-380 with a heat capacity of 6 kW is intended for backup (emergency) and peak heat supply in the event of the heat pump not being able to work or its insufficient heat output.

To conduct research on the effectiveness of the heat pump, the temperature of the heat carrier in the forward and return pipelines of both circuits is measured by TSP-002k type thermal sensors and recorded by secondary control devices. To automate the operation of the heat pump, following temperature sensors are used:

- heat carrier in the supply and return circuit of the heat pump with an intermediate heat carrier (supply and return heat carrier from the heat pump);
- heat carrier in the supply and return circuit of heating devices (supply and return heat carrier of the heating system);
- heat carrier in the supply and return circuit of the centralized heat supply system (supply and return heat carrier of the heating system);
- air inside the control room;
- external air.

Experimental studies, the results of which are presented, were conducted during the heating period in 2019 using different modes of operation of the heat supply system of a part of the administrative building using an air-water heat pump in different operating modes. The duration of the study of one of the modes was an average of 15 days.

With the help of the measuring complex, all the main heat supply parameters were determined and recorded automatically in real time at intervals from one to twenty minutes: the temperature of the heat carrier at the inlet and outlet of all circuits, the air in the control room and the environment, as well as the consumption of the heat carrier in each of the circuits.

Regulation of the heat pump operating modes was carried out using a temperature sensor installed on the return pipeline of the heat pump circuit. For a detailed analysis, time intervals of the heat supply system operation were chosen, during which the temperature of the surrounding air changed slightly and the process of heat transfer through the enclosing structures of the building was quasi-stationary.

### Study results and their discussion

In Figure 3 shows the experimental data that were obtained on January 24, 2019 from 5:00 a.m. to 11:00 a.m. The heat supply system based on the heat pump worked in the mode of heating 4 circuits of the heating devices of building No. 1, the peak electric boiler was turned off.

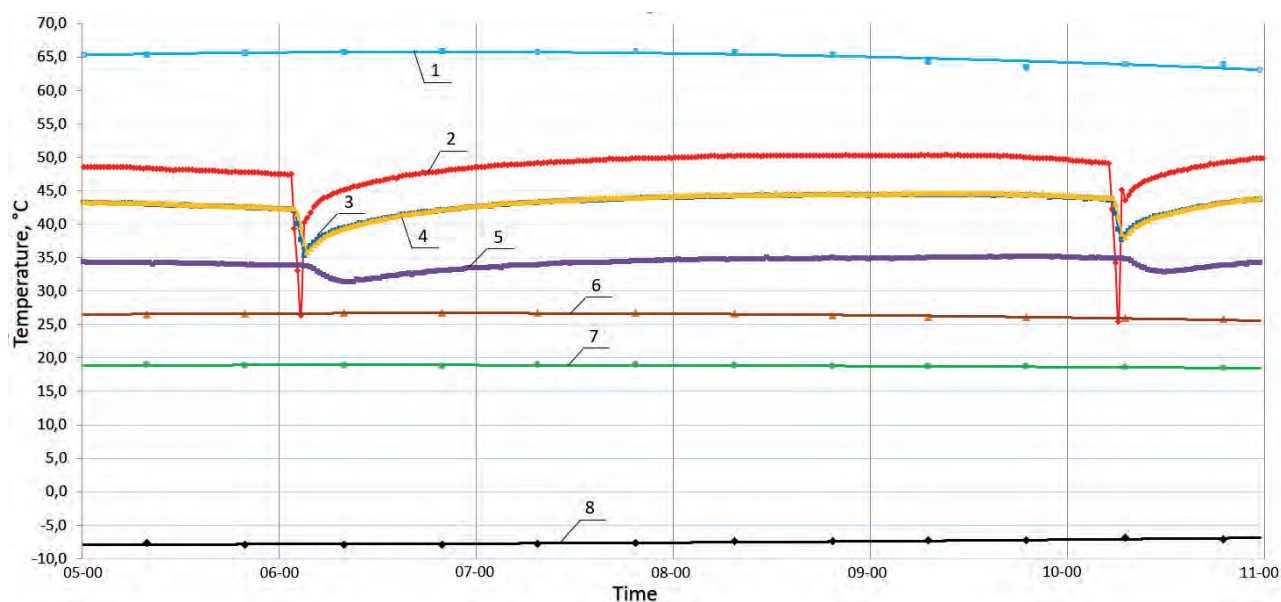


**FIGURE 3.** Dependencies of internal air and heat carrier temperatures in the circuits of the heat supply system of a part of the administrative building 24.01.2019 (hours): 1 – heat carrier supply temperature from the centralized heat supply system; 2 – the temperature of the intermediate heat carrier at the outlet of the heat pump; 3 – the temperature of the intermediate heat carrier at the inlet to the heat pump; 4 – the temperature of the heat carrier on supply to the heating system; 5 – temperature of the return heat carrier from the heating system; 6 – the temperature of the return heat carrier of the centralized heat supply system; 7 – air temperature in the control room; 8 – outdoor air temperature

The flow of the heat carrier was:

- heat carrier flow in the centralized heat supply system  $G_1 = 1.1-1.3 \text{ m}^3/\text{h}$ ;
- heat carrier flow in the circuit of the heat pump  $G_{\text{TN}} = 1.2 \text{ m}^3/\text{h}$ ;
- heat carrier flow in the  $G_{\text{CO}}$  heating system =  $1.4 \text{ m}^3/\text{h}$ .

As can be seen from Figure 3, the heat pump operates with an on/off interval of about 4 hours, indicating an excessive heat load on the heating system. The temperature of the heat carrier supplied to the heating system is on average  $0.5^\circ\text{C}$  lower than the temperature of the return heat carrier of the heat pump circuit. This indicates the insufficiency of the available heat exchange surface and the need to increase it. The outside air temperature ranged from  $-7.7^\circ\text{C}$  to  $-7.1^\circ\text{C}$ . The internal air temperature was within  $19.0^\circ\text{C} \pm 0.5^\circ\text{C}$ .

Based on the obtained experimental data, the coefficient of performance (COP) of the heat pump was calculated for the above mode of operation of the heat supply system, which was  $\text{COP}_1 = 1.6$ .

In Figure 4 shows the experimental data obtained on February 25, 2019 from 17:00 to 23:00. The heat supply system based on the heat pump worked in the mode of heating 4 circuits of the heating devices of the building No. 1, the peak electric boiler heated up the heat carrier of the circuit of the heating system of the building. The flow of the heat carrier was:

- heat carrier flow in the centralized heat supply system  $G_1 = 1.2-1.3 \text{ m}^3/\text{h}$ ;
- heat carrier flow in the circuit of the heat pump  $G_{\text{TN}} = 0.95 \text{ m}^3/\text{h}$ ;
- heat carrier flow in the  $G_{\text{CO}}$  heating system =  $1.75 \text{ m}^3/\text{h}$ .

The heat pump operation interval in this mode decreased and the on/off period was 1.5 hours. In this operating mode, the temperature of the heat carrier that was supplied to the heating system is on average  $3.0-3.5^\circ\text{C}$  higher than the temperature of the return heat carrier of the heat pump circuit due to the operation of the electric boiler. The outside air temperature ranged from  $-5.3^\circ\text{C}$  to  $-4.1^\circ\text{C}$ . The internal air temperature was  $19.5^\circ\text{C}$ .

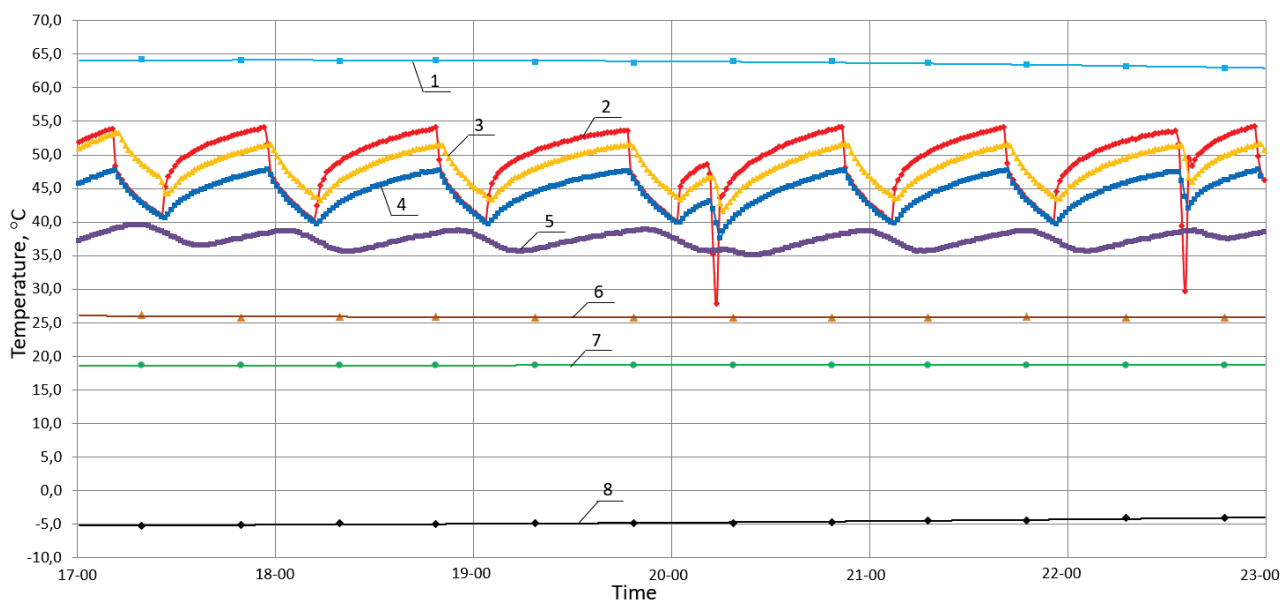


**FIGURE 4.** Dependencies of internal air and heat carrier temperatures in the circuits of the heat supply system of a part of the administrative building 25.02.2019 (hours): 1 – heat carrier supply temperature from the centralized heat supply system; 2 – the temperature of the intermediate heat carrier at the outlet of the heat pump; 3 – the temperature of the intermediate heat carrier at the inlet to the heat pump; 4 – the temperature of the heat carrier supply to the heating system; 5 – temperature of the return heat carrier from the heating system; 6 – the temperature of the return heat carrier to the centralized heat supply system; 7 – air temperature in the control room; 8 – outdoor air temperature



At 20: 15 and 22:40 there is a sharp decrease in the temperature of the supply heat carrier of the circuit of the heat pump, which is explained by icing of the surface of the evaporator of the heat pump.

The COP of the heat pump was calculated for the above mode of operation of the heat supply system, which was  $COP_2 = 1.62$ . A slight increase of the  $COP_2$  is explained by a relatively high value of the outside air temperature.

In Figure 5 shows the experimental data obtained on March 4, 2019 from 12:00 to 18:00. The heat supply system based on the heat pump worked in the mode of heating 6 circuits of the heating devices of building No. 1, the peak electric boiler was turned off. The flow of the heat carrier was:

- heat carrier flow in the centralized heat supply system  $G_1 = 0.9-1.2 \text{ m}^3/\text{h}$ ;
- heat carrier flow in the circuit of the heat pump  $G_{TN} = 0.75 \text{ m}^3/\text{h}$ ;
- heat carrier flow in the  $G_{CO}$  heating system =  $2.1 \text{ m}^3/\text{h}$ .

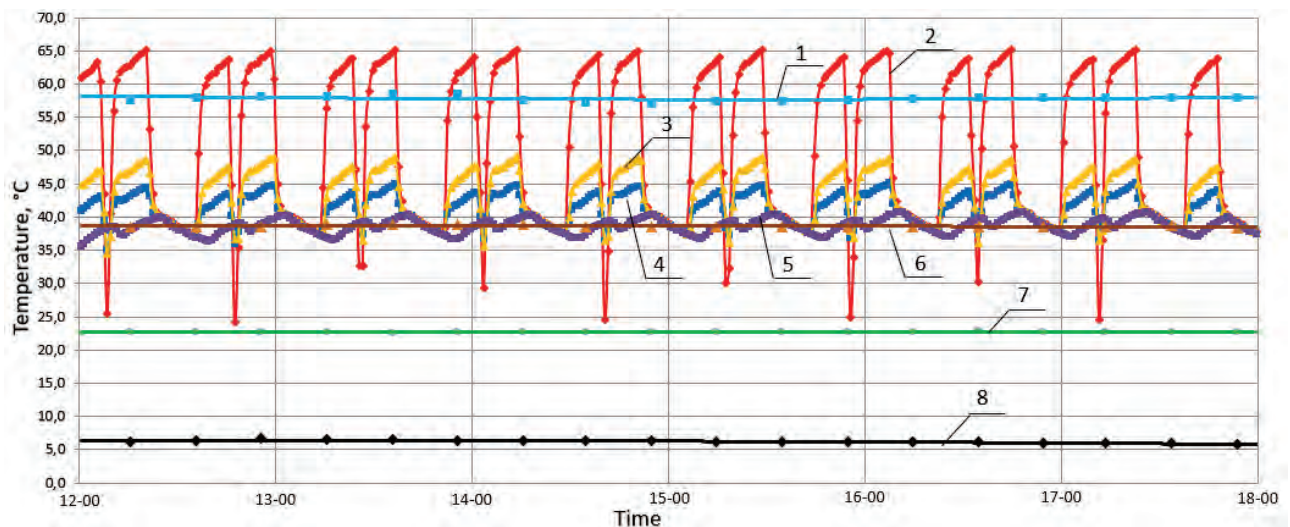


**FIGURE 5.** Dependencies of internal air and heat carrier temperatures in the circuits of the heat supply system of a part of the administrative building 03.04.2019 (hours): 1 – heat carrier supply temperature from the centralized heat supply system; 2 – the temperature of the intermediate heat carrier at the outlet of the heat pump; 3 – the temperature of the intermediate heat carrier at the inlet of the heat pump; 4 – the temperature of the heat carrier supply to the heating system; 5 – temperature of the return heat carrier from the heating system; 6 – the temperature of the return heat carrier to the centralized heat supply system; 7 – air temperature in the control room; 8 – outdoor air temperature

The heat pump operation interval in this mode decreased and the on/off period was 45 minutes. In this mode of operation, the temperature of the heat carrier supplied to the heating system is on average  $5.0^{\circ}\text{C}$  higher than the temperature of the return heat carrier of the heat pump circuit due to the reduction of heat losses of the building and the increase of the heat carrier temperature. The outside air temperature ranged from  $6.1^{\circ}\text{C}$  to  $6.5^{\circ}\text{C}$ . The internal air temperature rose to  $22.8^{\circ}\text{C}$ .

In this mode of operation, icing of the surface of the evaporator occurs in almost every cycle of the heat pump, which negatively affects the resource of the heat pump and reduces the reliability of the entire heat supply system.

Based on the obtained experimental data, the COP of the heat pump was calculated for the above mode of operation of the heat supply system, which was  $COP_3 = 1.94$ . An even greater value can be explained by the increase in the temperature of the outside air and the decrease in the limit value of the coolant temperature in the circuit of the heat pump.



## Conclusion

Average for the heating period, the COP of the air-water heat pump, when it was integrated into the existing heat supply system of the administrative energy building, was  $COP = 1.82$ , which is significantly less than the recommended 2.5-2.7 for proper implementation. However, even with such indicators, a significant saving of thermal energy is achieved, from 10% to 24%, in comparison with the use of a centralized heat supply system.

## References

- [1] Dolinskyi A.A., Basok B.I., Ye. T., 2015, *Bazieiev Enerhetychna stratehiia Ukrainy: rozvytok teplozabezpechennia*. Promyshlennaia teplotekhnika. Vol. 37, No. 2, pp. 3-11. <https://doi.org/10.31472/ihe.2.2015.01>.
- [2] Ibrahim O., Fardoun F., Younes R., Louahlia-Gualous H., 2014, *Review of water-heating systems: General selection approach based on energy and environmental aspects*. Building and Environment. Vol. 72, pp. 25-286. <https://doi.org/10.1016/j.buildenv.2013.09.006>.
- [3] Mazurenko A.S., Klymchuk A.A., Yurkovskiy S.Iu., Omeko R.V., 2015, *Razrabotka skhemy kombynyrovanoi systemy teplosnabzheniya s yspolzovanyem sezonnoho akkumulyrovanyia tepla ot helyosystem*. Vostochno-Evropeyskyi zhurnal peredovykh tekhnolohiy. No. 8 (73), pp. 17-20. <https://doi.org/10.15587/1729-4061.2015.36902>
- [4] Fong K.F., Chow T.T., Hanby V.I., 2006, *Development of Optimal Design of Solar Water Heating System by Using Evolutionary Algorithm*. Journal of Solar Energy Engineering. No. 4, Vol. 129. <https://doi.org/10.5862/MCE.58.4>.
- [5] Alihodzic R., Murgul V., Vatin N., Aronova E., Nikolić V., Tanić M., Stanković D., 2014, *Renewable energy sources used to supply pre-school facilities with energy in different weather conditions*. Applied Mechanics and Materials. Vol. 624, pp. 604-612. <https://doi.org/10.4028/www.scientific.net/AMM.624.604>.
- [6] Basok B.I., Bieliaieva T.H., Koba A.R., Tkachenko M.V., Nedbailo O.M. ta insh., 2009, *Kompleksna modernizatsiia typovoi systemy teplopostachannia budivli na osnovi vykorystannia teplovoho nasosu typu «povitria-voda»*. Promyshlennaia teplotekhnika. Vol. 31. No. 7, pp. 19-21.
- [7] Nedbailo O.M., 2010, *Vykorystannia teplovoho nasosu typu «povitria-ridyna» v isnuiuchii tsentralizovanii systemi opalennia*. Kompresornoe y enerhetycheskoe mashynostroenye. No. 2(20), pp. 32-36.
- [8] Basok B.I., Nedbailo O.M., Tkachenko M.V., Bozhko I.K., Lysenko O.M., Lunina A.O., 2015, *Modernizatsiia systemy opalennia budivli z vykorystanniam teplovoho nasosa typu «povitria-ridyna»*. Promyshlennaia teplotekhnika. Vol. 37, No. 5, pp. 68-74. <https://doi.org/10.31472/ihe.5.2015.08>.

Andrii CHEILYTKO

German Aerospace Center (DLR),

Institute of Solar Research, Julich, Germany

Corresponding author: andrii.cheilytko@dlr.de

Doi: 10.53412/jntes-2022-3-4

## INFLUENCE OF STRUCTURAL CHARACTERISTICS OF POROUS MATERIALS ON THE COEFFICIENT OF THERMAL CONDUCTIVITY

**Abstract:** *The existing dependences of the effective coefficient of thermal conductivity of the material depending on the size and location of pores in it are analyzed and compared with each other and with previously obtained experimental data. It is shown that the resulting thermophysical properties of the material are affected not only by the porosity, but also by the location of the pores in the volume of the material. The disadvantages of the existing dependences of determining the effective thermal conductivity of the material on the type of porosity (both for porous material and for dispersed systems) are shown. Also, the most reliable dependences of the thermal conductivity coefficients on the porosity of dispersed systems for backfill materials and the need for their correction by empirical coefficients are determined.*

*Complex indicators that fully describe the porous structure and on which the mathematical model of heat exchange processes in a porous medium should be based are proposed.*

**Keywords:** *porous media, heat transfer, effective thermal conductivity coefficient, thermal resistance*

### Introduction

Porous materials are widely used in industry. These are polystyrene foam materials, aerated concrete, some highly fire-resistant materials, foam glass, expanded clay. Porous materials have also occupied a niche in innovative technologies: combustion chambers, turbine walls, solar station receivers, thermal storage.

If we consider porous materials as dispersed systems, the main mechanism of heat transfer is, of course, the thermal conductivity of the material itself (the skeleton of the dispersed system) and the thermal conductivity of the medium in the pore (Hamdami et al., 2004). To calculate the thermal conductivity, a formal analogy between the basic laws of electricity and heat (the theory of generalized conductivity) is often used (Liang et al., 2013). However, it has been experimentally proved that when calculating the thermal conductivity of a porous material according to Maxwell's theory or Rayleigh's theory (calculation of the electric field of a system in which foreign particles of spherical shape are embedded), there is a significant discrepancy between the theoretically determined coefficient of thermal conductivity of a porous material and the actual one (Liang et al., 2013). Most likely, the discrepancy between theory and experiment is due to the idealization of model structures (Liang et al., 2013). There are also quite a number of other works (Säckel and Nieken, 2016; Lowell and Shields, 2016), in which it is stated that the generalized theoretical justification of the thermal conductivity of porous material gives differences with the experiments. Also, convection in the pores of thermal insulation products will depend on the operating conditions (Pavlenko, 2014). Therefore, it is necessary to understand how the porous structure affects the thermophysical properties of the material under different conditions of its operation, such as: temperature; dynamics of temperature

change; duration of its exposure; humidity and others. Therefore, a working hypothesis of controlled structure formation of materials and the formation of its thermophysical properties was formed.

**Working hypothesis:** the influence of structural parameters on the thermophysical characteristics of the material allows to create a theoretical basis for the controlled structure formation of heat-insulating mats with specified thermophysical properties.

To confirm the working hypothesis, we consider the influence of structural parameters on the thermophysical characteristics of the material.

### **Statement of the problem**

The thermal properties of thermal insulation materials and thermal protection structures will be affected by micropores, mesopores, macropores, cavities, voids and structural channels.

As mentioned above, as the pore size in materials and products increases above 0.1 mm, the effective thermal conductivity of the material due to convection increases. Heat transfer due to radiation with increasing optical path thickness decreases exponentially, but with increasing pore size, the radiation surface area also increases, which increases the radiation component (Zhang et al., 2015). Therefore, the effect of radiation on the flow of heat through the porous structure of thermal protection of power equipment when changing the shape and size of the pores is a dependence that should be considered as part of the generalized equation of the effective thermal conductivity of porous heat-insulating materials on the complex parameters of the porous structure. One of the complex indicators of the porous structure of the material or structure is the shape of the pore. The effective thermal conductivity coefficient for a material with pores oriented along the heat flow is almost twice as high as for a material with pores oriented perpendicular to the heat flow (Fugallo et al., 2014). This difference is the greater, the larger the pore size. Thus, the pore size is the second complex indicator of the porous structure.

### **Analysis of main studies and publications on the problem**

Experimental data, both research and production, on optimum conditions of bloating are also different, since there is no theory generalizing the physical processes that occur during the formation of porosity. For example, preheating of bloating initial mixture of cellular glass to sintering temperature (690°C) is recommended as 70 minutes or 15 minutes.

All this proves that the porosity of the material plays an essential role in the thermophysical characteristics of the material.

As the pore size increases, the conduction of heat through convection increases. An increase in pore size has a similar effect on the radiative component.

### **Results of research**

Let's take a closer look at the effect of pore location on the thermal conductivity of the material. Table 1 uses the following designations: porosity,  $\lambda_1$  – heat transfer coefficient of the material (silica material with a heat transfer coefficient of 0.12 W/(m·K) was chosen as an example)  $\lambda_2$  is the thermal conductivity coefficient of the medium (in the example selected air with gas admixtures having a thermal conductivity of 0.019 W/(m·K)). Heat flow is directed from the bottom upwards. The black color indicates the material.

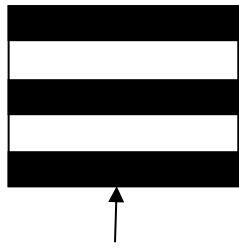
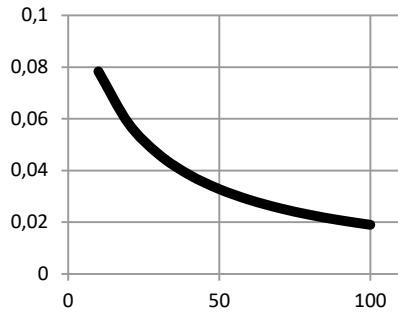
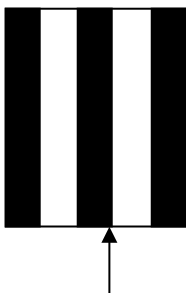
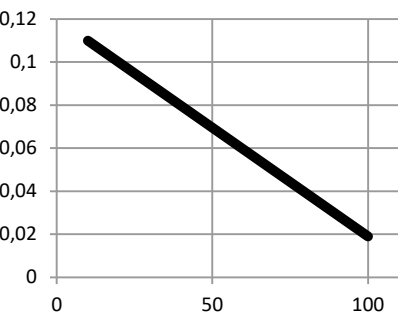
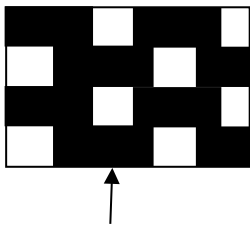
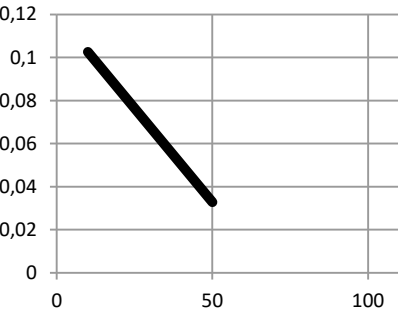
The formula derived by Aiken also applies to the calculation of the thermal conductivity of fill (No. 8 and No. 9 in Table 1):

$$\lambda_{ef} = \frac{\lambda_1 + 1 + \frac{2p \left(1 - \frac{\lambda_1}{\lambda_2}\right)}{2\lambda_1 - 1}}{\lambda_2} \cdot \frac{1 - \frac{\lambda_1}{\lambda_2}}{1 - p \frac{2\lambda_1 + 1}{\lambda_2}}$$

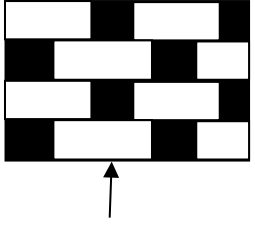
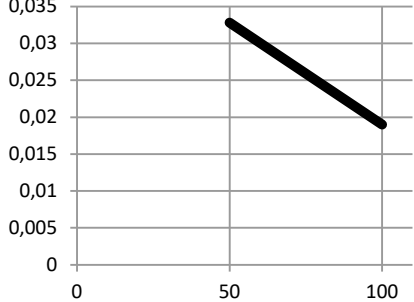
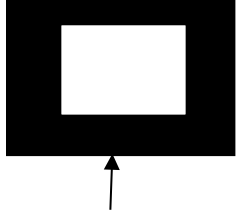
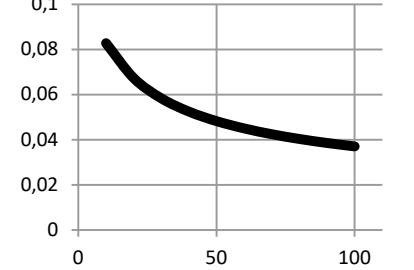
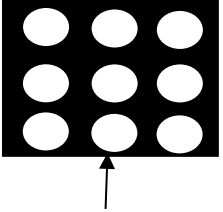
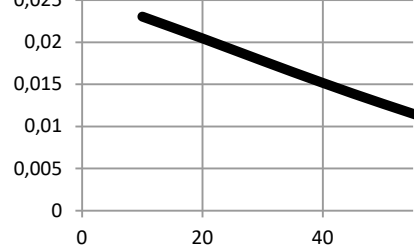
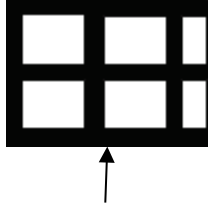
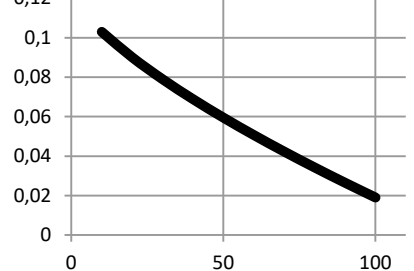
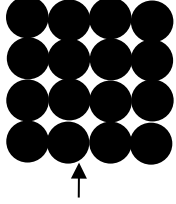
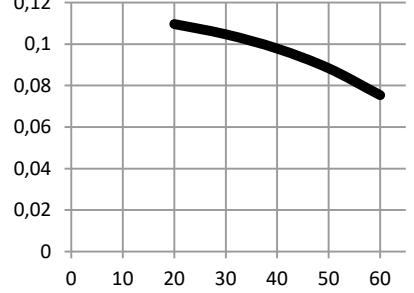
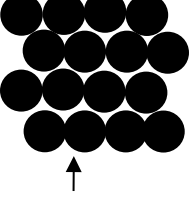
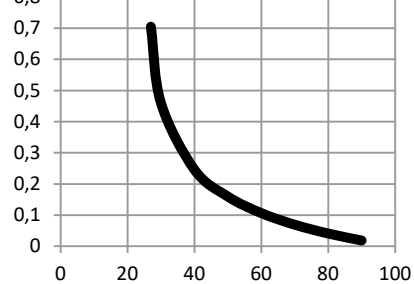
and Torcar's formula

$$\lambda_{ef} = \frac{\lambda_1}{1-p}$$

**TABLE 1.** Summary of dependencies of the thermal conductivity coefficient on porosity for two-phase systems

No.	Pore layout Formula for calculating the effective thermal conductivity coefficient	Pore layout Formula for calculating the effective thermal conductivity coefficient	Example $\lambda_{ef} = f(p)$
1		$\lambda_{ef} = \lambda_2 \frac{100}{\frac{\lambda_2}{\lambda_1}(100-p) + p}$	
2		$\lambda_{ef} = \lambda_1 \frac{100-p}{100} + \lambda_2 \frac{p}{100}$	
3		$\lambda_{ef} = \lambda_2 \left[ \frac{4p}{1 + \frac{\lambda_2}{\lambda_1}} + \frac{\lambda_1}{\lambda_2} (1-2p) \right]$ if $p \leq 50\%$	



4		<p>if <math>p \geq 50\%</math></p> $\lambda_{ef} = \lambda_2 \left[ \frac{4(1-p)}{1 + \frac{\lambda_2}{\lambda_1}} + (2p-1) \right]$	
5		$\lambda_{ef} = \frac{\lambda_1^2 p^{\frac{2}{3}} + \lambda_1(\lambda_2 - \lambda_1)}{\lambda_1 + p^3(\lambda_2 - \lambda_1)}$	
6		<p>if <math>p \leq 50\%</math></p> $\lambda_{ef} = \frac{\lambda_2 p + \frac{\lambda_2}{\lambda_1} \left( 1 - p^{\frac{2}{3}} \right)}{p - p^3 \frac{\lambda_1}{\lambda_2} \left( 1 - p^{\frac{2}{3}} + p \right)}$	
7		$\lambda_{ef} = \lambda_2 p^3 + \lambda_1 (1-p)^{\frac{2}{3}}$	
8		<p><math>p \approx 48\%</math></p> $\lambda_{ef} = \frac{1.5\pi\lambda_1(0.9-p)}{(2.1-p)^2}$	
9		<p><math>p \approx 30\%</math></p> $\lambda_{ef} = 3\pi\lambda_1 \ln \frac{43 + 0.31p}{p - 26}$	

Aiken's formula gives the smallest error for particle shapes approaching a sphere and for porosity less than 50%. For dispersed material backfill, case No. 9 in Table 1 is the most appropriate.

For granular silica backfills it is recommended to use the Odelevsky formula:

$$\lambda_{ef} = \lambda_1 \left( 1 + \frac{p_1}{\frac{1-p_2}{3} + \frac{\lambda_1}{\lambda_2 - \lambda_1}} \right)$$

Using Table 1, graphical analysis of formulas for calculating the thermal conductivity of porous materials (Fig. 1) and separately for the backfill (Fig. 2). For the porous material we leave the same values of thermal conductivity as in the example, and for the backfill of solid phase we take the thermal conductivity equal to granules of thermal insulation material based on silica for medium-temperature insulation (0.036 W/(m·K)) (Pavlenko, 2020).

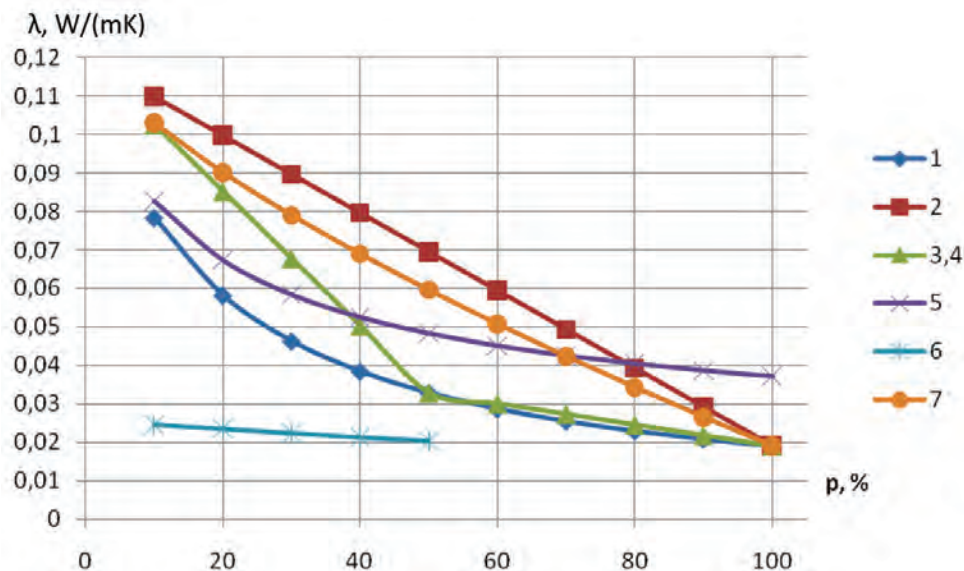


**FIGURE 1.** Influence of porosity on the effective heat transfer coefficient for different schemes of porosity according to Table 1

Structures 1 and 2 are given as the maximum and minimum teleretic values of the effective thermal conductivity and set the limits of the study.

As can be seen from Figure 1, the structure No. 6 with the calculated formula underestimates the value of the thermal conductivity coefficient, and at a porosity of 10% the thermal conductivity coefficient of the material cannot be approximately equal to the thermal conductivity coefficient of air. Therefore, the calculation formula No. 6 is not correct for these ratios of the coefficients of thermal conductivity of air and material.

Calculation formula No. 5 does not take into account the influence of pore size, or rather it was considered by the author as a large structure. Also, contrary to logic, the values of thermal conductivity in No. 5 are underestimated at porosity up to 30%.

As can be seen from Figure 2, the formula of Aiken and Bogomolov (No. 9 of Table 1) shows only a general dependence and needs empirical correction. The Torkar and Odelevsky dependencies express an increase in the coefficient of thermal conductivity with an increase in porosity and are suitable only for moist disperse systems or systems with large pore sizes. Nekrasov's dependence for an idealized structure (No. 8 of Table 1) is the most acceptable.

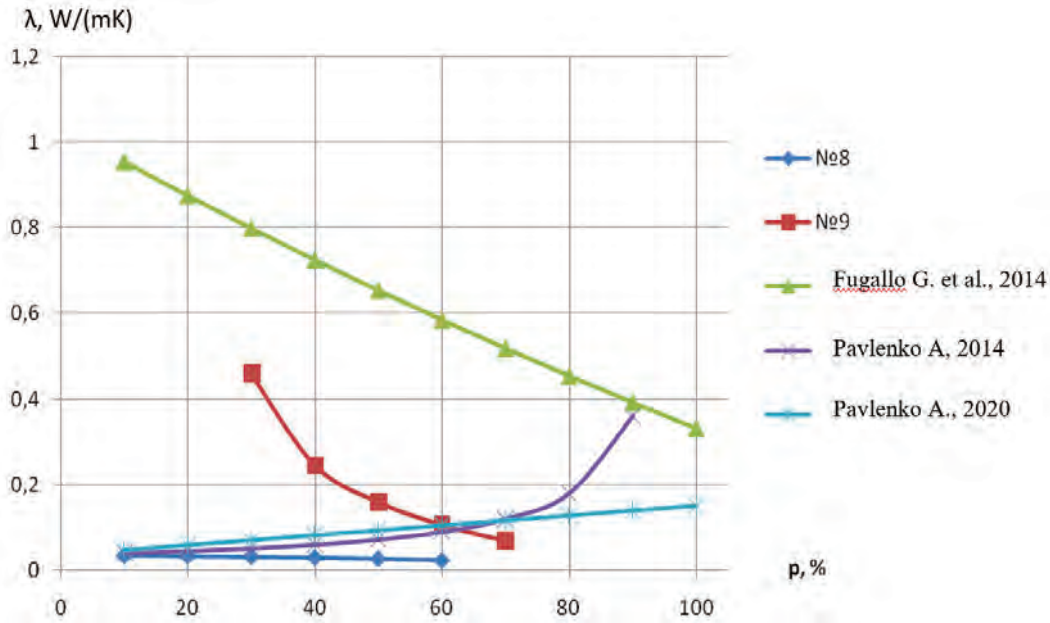


FIGURE 2. Effect of porosity on the effective coefficient of thermal conductivity for fillings of dispersed material according to Table 1

The formula for calculation of channel porosity in absorbers was also derived. The mathematical model of the proposed equation was based on a conditional isothermal channel with additional resistance to fluctuations in the direction of the dislocation vector.

Let us calculate the resistance of displacement vectors by the method of electrothermal analogy, for two-dimensional space in the direction of the structure vectors for a chaotic structure of the first order. In this case, we assume that the  $x$  direction in which the heat flow passes in the higher scale structure can be decomposed into  $x$  and  $y$  vectors in the lower scale structure:

$$R_{xj} = \sum_{i=1}^{n_1} R_{xj_i}, j = 1, 2$$

$$R_{xj_i} = R_f + R_s$$

$$R_{x1} = n_x \frac{d_x}{\lambda_f} + \frac{n_x (r_x - d_x)}{\lambda_s}$$

$$R_{x2} = n_y \frac{d_2}{\lambda_f} + \frac{n_y (r_y - d_2)}{\lambda_s}$$

$$R_{x1} = \frac{n_x d_x \lambda_s + \lambda_f k_x l_x - \lambda_f n_x d_x}{\lambda_s \lambda_f}$$

$$R_{x2} = \frac{n_y d_2 \lambda_s + \lambda_f k_y l_y - \lambda_f n_y d_2}{\lambda_s \lambda_f}$$

$$\frac{1}{R} = \frac{1}{R_{x1}} + \frac{1}{R_{x2}}$$

So

$$\begin{aligned}
 R &= \frac{\left( \frac{n_x d_x \lambda_s + \lambda_f k_x l_x - \lambda_f n_x d_x}{\lambda_s \lambda_f} \right) \left( \frac{n_y d_2 \lambda_s + \lambda_f k_y l_y - \lambda_f n_y d_2}{\lambda_s \lambda_f} \right)}{\left( \frac{n_x d_x \lambda_s + \lambda_f k_x l_x - \lambda_f n_x d_x}{\lambda_s \lambda_f} \right) + \left( \frac{n_y d_2 \lambda_s + \lambda_f k_y l_y - \lambda_f n_y d_2}{\lambda_s \lambda_f} \right)} \\
 &= \frac{(n_x d_x \lambda_s + \lambda_f k_x l_x - \lambda_f n_x d_x)(n_y d_2 \lambda_s + \lambda_f k_y l_y - \lambda_f n_y d_2) \left( \frac{1}{\lambda_s \lambda_f} \right)}{n_x d_x \lambda_s + \lambda_f k_x l_x - \lambda_f n_x d_x + n_y d_2 \lambda_s + \lambda_f k_y l_y - \lambda_f n_y d_2} \\
 &= \frac{(n_x d_x \lambda_s + \lambda_f k_x l_x - \lambda_f n_x d_x)(n_y d_2 \lambda_s + \lambda_f k_y l_y - \lambda_f n_y d_2)}{\lambda_s \lambda_f (n_x d_x \lambda_s + \lambda_f k_x l_x - \lambda_f n_x d_x + n_y d_2 \lambda_s + \lambda_f k_y l_y - \lambda_f n_y d_2)}
 \end{aligned}$$

If there is no displacement in the x-axis  $k_x = 1$

$$R = \frac{(n_x d_x \lambda_s + \lambda_f l_x - \lambda_f n_x d_x)(n_y d_2 \lambda_s + \lambda_f k_y l_y - \lambda_f n_y d_2)}{\lambda_s \lambda_f (n_x d_x \lambda_s + \lambda_f l_x - \lambda_f n_x d_x + n_y d_2 \lambda_s + \lambda_f k_y l_y - \lambda_f n_y d_2)}$$

For an open porous structure will be true  $n_x d_x = l_x$

$$R = \frac{(l_x \lambda_s + \lambda_f l_x - \lambda_f l_x)(n_y d_2 \lambda_s + \lambda_f l_y k_y - \lambda_f n_y d_2)}{\lambda_s \lambda_f (n_x d_x \lambda_s + \lambda_f l_x - \lambda_f l_x + n_y d_2 \lambda_s + \lambda_f k_y l_y - \lambda_f n_y d_2)}$$

Porosity in the direction of the radius vector

$$\varnothing' = \frac{n_y d_2}{k_y l_y}$$

$$R = \frac{l_x (\lambda_s \varnothing' k_y l_y + k_y l_y \lambda_f (1 - \varnothing'))}{\lambda_f (\lambda_s (n_x d_x + \varnothing' k_y l_y) + \lambda_f k_y l_y (1 - \varnothing'))}$$

$$R = \frac{l_x (\lambda_s \varnothing' + \lambda_f (1 - \varnothing'))}{\lambda_f \left( \lambda_s \left( \frac{n_x d_x}{k_y l_y} + \varnothing' \right) + \lambda_f (1 - \varnothing') \right)}$$

$$\lambda_{\text{vector}_f} = \lambda_f \frac{\lambda_s \frac{l_x}{k_y l_y} + \lambda_s \varnothing' + \lambda_f (1 - \varnothing')}{\lambda_s \varnothing' + \lambda_f (1 - \varnothing')}$$

$$\lambda_{\text{vector}_f} = \lambda_f \left[ 1 + \frac{\lambda_s \frac{l_x}{k_y l_y}}{\lambda_s \varnothing' + \lambda_f (1 - \varnothing')} \right]$$

The above formula requires similar transformations with the thermal conductivity of a solid. After that, it is necessary to convert the xy space into a single vector of the heat flux direction to obtain the desired function.



## Complex indicators of porous structure

Most of the existing studies of porous structures of materials for thermal protection of elements of industrial power plants take into account the total porosity as the main structural characteristic of the thermal insulation material, and sometimes take into account either the shape of the pores and their number or the type of pores (Rudobashta et al., 2015). The analysis of the current literature shows that even the simultaneous consideration of the total porosity of the material, the size and type of pores is not enough to fully characterize the porous structure of the heat-insulating material. In (Rudobashta et al., 2015), it is proposed to pay attention to the following main factors in porous systems: the nature of the structure, the number of structure components, the aggregate state of the structure components and the processes of interaction between the structure components. These complex indicators are convenient for the separation of porous systems as a whole because they allow controlling the thermophysical properties of a particular macroporous material by changing the porosity structure. But these indicators do not allow to find the functional dependence of the thermophysical properties of heat-insulating materials on the porous structure, which does not allow to optimize the thermophysical properties of porous heat-insulating material by creating predictable porous structures. Therefore, we propose the main complex indicators of the porous structure of the heat-insulating material and structures of thermal protection of elements of industrial power plants, which fully reflect the porous structure and make it possible to draw up a regression equation for the dependence of the thermal properties of porous heat-insulating materials on the proposed indicators:

1. Porosity  $P$ , % – porosity as a general indicator of the density of thermal insulation material and thermal protection structures.
2. Number of pores  $n$ , pcs/m<sup>3</sup> – the number of pores for a homogeneous structure in combination with porosity gives a general idea of the distribution of pores in the material. The change in the number of pores over time during the formation of the porous structure of heat-insulating materials expresses the dynamics of the pore formation process.
3. The location of the pores in space – described by the Bravais translation system (Bravais lattice), in which the pore is the core of the lattice with dimensions smaller than the Wigner-Seitz cell, or the statistical distribution of pores in the volume of the insulating material.
4. Pore shape – a spatial coordinate function describing the shape of the pore. It is possible to accept the description of all pores as spheres with the description of the deformation inherent in this sphere, according to the Poincaré hypothesis, or the overall dimensions of the pore, or the general coefficient of geometric characteristics of the porous structure.
5. Indicators of the gas state in the pores – the temperature gradient on which convection in the pores and the physical properties of the coolant in the pore depend. It can also be represented by the product of Grashof number and Prandtl number.
6. Specific surface area porosity  $S$ .

To determine the energy intensity of the created porous thermal insulation materials and structures of thermal protection of elements of industrial power plants, the energy of formation of the porous structure is used:

$$dQ_{por} = T_{por}dS + \varphi_{por}dM_{por}$$

## Conclusion

The closest to minimally thermally conductive (theoretical) structure is the staggered arrangement of pores stretched perpendicular to the heat flow over the volume. This is also confirmed by experimental studies.

After analyzing Figure 2 it can be concluded that for the idealized case of fill with total porosity of about 50% the effective thermal conductivity coefficient can be calculated with the help of Nekrasov's

dependence (No. 8 of Table 1). For practical calculations (porosity of disperse system is about 30%), it is necessary to correct Bogomolov's dependence by empirical coefficients (No. 9 of Table 1).

Complex indicators that fully describe the porous structure and on which the mathematical model of heat exchange processes in a porous medium should be based are proposed: porosity, number of pores, the location of the pores in space, pore shape, indicators of the gas state in the pores.

### References

- Hamdami N., Monteau J.-Y., Bail A.L., 2004, *Transport properties of a high porosity model food at above and sub-freezing temperatures*. Pt 1. Properties and water activity, J. Food Eng., vol. 62, No. 4, pp. 373-383.
- Liang Y., Wu D., Fu R., 2013, *Carbon microfibers with hierarchical porous structure from electrospun fiber-like natural biopolymer*. Scientific reports. T. 3, p. 1119.
- Lowell S., Shields J.E., 2013, *Powder surface area and porosity*. Springer Science & Business Media, T. 2.
- Fugallo G. et al., *Thermal conductivity of graphene and graphite: collective*.
- Pavlenko A., Deshko V.I., Cheilytko A.O., Sukhodub I., 2020, *Efficiency of using energy in the housing sector*, monografie. Kielce University of Technology. 147 p.
- Pavlenko A., 2014, *Basis of forming pores in the material based on argil and their effect on thermal conductivity*.
- Pavlenko A., Cheilytko A., Energy saving and ration Nature Use. Kazimierz Pułaski University of Technology and Humanities in Radom, Poltava National Technical Yuri Kondratyuk University. No. 2(3), pp. 81-84.
- Rudobashta S.P., Zueva G.A., Zuev N.A., 2015, *Hygroscopic Properties of Seeds*. Izvestiya Vysshikh Uchebnykh Zavedenii. Seriya Khimiya i Khimicheskaya Tekhnologiya. T. 58. No. 1.
- Säckel W., Nieken U., 2016, *Structure Formation within Spray-Dried Droplets; Mathematical Modelling of Spray Polymerisation*. Process-Spray. Springer International Publishing, pp. 89-125.
- Zhang C. et al., 2015, *MHD flow and radiation heat transfer of nanofluids in porous media with variable surface heat flux and chemical reaction*. Applied Mathematical Modelling. T. 39. No. 1, p. 165-181.